Pergamon

Journal of Structural Geology, Vol. 16, No. 6, pp. 839 to 852, 1994
Elsevier Science Ltd
Printed in Great Britain
0191-8141/94 $07.00+0.00

Strain patterns within the late Variscan granitic dome of Velay, French Massif Central

JEAN-LOUIS LAGARDE and CHRISTOPHE DALLAIN*

"Géosciences Rennes", 35042 Rennes Cédex, France

and

PATRICK LEDRU and GABRIEL COURRIOUX

BRGM-SGN, 45060 Orléans, France

(*Received* 10 *December* 1991; *accepted in revised form* 14 *July* 1993)

Abstract—The Velay granites are intruded as a late Variscan dome in the French Massif Central. Strain patterns within the Velay granites reflect the geometry and kinematics of late Carboniferous deformation, at the site of final emplacement. The internal deformation developed during granitic magmatism is not homogeneously distributed. From inner to outer zones increasing deformation is marked by changes from high-temperature foliations to *S–C* orthogneisses. Strain concentration at the margins reflects a strength contrast due to cooling and subsequent magma hardening. According to the internal strain field two zones can be distinguished in the Velay dome: (i) a central and southern zone where concentric patterns indicate a southward expansion of granites; and (ii) a northern zone where the lateral expansion is limited and combined with top-to-the-north extensional shearing along the Mont Pilat detachment zone and high-temperature wrenching. These asymmetric strain patterns relate to the expansion and deformation of granites emplaced below a detachment fault, during the uplift of a thickened area. Post-thickening combination of extensional and wrench tectonics is inferred.

INTRODUCTION

THE tectonic setting of late Variscan crustal anatexis in western Europe is a much debated problem. Most of the late Variscan granitoids are late Carboniferous in age (Vidal 1980, Duthou *et al.* 1984), i.e. emplaced 40–100 Ma after the Variscan thickening (Burg 1983, Matte 1991). They consist of post-thickening, collision-related granites and they show various indicators of syn to late tectonic emplacement at shallow crustal levels (Lagarde *et al.* 1992). Within the little deformed foreland areas, as exemplified by the Moroccan meseta and Central Brittany, granitoids record extensive, crustal-scale wrenching active during late convergence (Berthé *et al.* 1979, Grapais & Le Corre 1980, Lagarde *et al.* 1990a, Hutton & Reavy 1992). Within the thickened internides as exemplified by Southern Brittany and the French Massif Central, most of the late Carboniferous granitoids consist of highly peraluminous monzogranites that post-date the early thrusts and the early high pressure eclogitic deformation (Burg 1983). Some of them have accumulated within large granitic and gneissic domes such as the Velay and the Montagne Noire (Fig. 1b). Their tectonic significance is debated: were these anatectic granites emplaced: (i) during crustal-scale wrenching, at the end of the Variscan continental collision, as in the Variscan externides (Lagarde *et al.* 1990a); (ii) during a syn-convergence extension, following the Himalayan model (Burg *et al.* 1984, Gapais *et al.* 1992); or (iii) during a post-collisional extension (Malavielle *et al.* 1990, Van Den Driessche & Brun 1992). Deformation analysis within the Velay granitic dome provides some useful constraints for such discussion.

In this paper microstructural changes of granites are described in order to determine the relationship between foliation development and granite emplacement. Then, strain patterns in the Velay dome are used to establish geometry and kinematics of granite deformation at the site of final emplacement. Finally, the tectonic setting of the late Variscan anatexis is discussed in the light of the new data presented.

GRANITES OF THE VELAY

The Velay granites have accumulated in a hectokilometric granitic and gneissic dome of the Massif Central (Dupraz & Didier 1988) (Fig. 1). Magmatism took place during late Variscan (Hercynian) anatexis, 300 Ma ago (Caen-Vachette *et al.* 1982), about 60–80 Ma after the onset of Variscan thickening in the Upper Devonian (Matte 1991). The granites crop out within low-pressure, high-temperature metamorphic rocks, previously underthrusted to the north along a major Variscan thrust of the French Massif Central (Burg 1983). Granites post-date this Variscan thrust. Wall-rocks, below the Variscan thrust, consist of migmatitic paragneiss and orthogneiss. The overlying unit contains dry and competent granulites, eclogites and high-grade gneisses inherited from the thickening episode (Burg 1983, Gardien 1990).

Granites in the Velay dome consist of highly peralu-

*Also at: BRGM-SGN, 45060 Orléans, France.

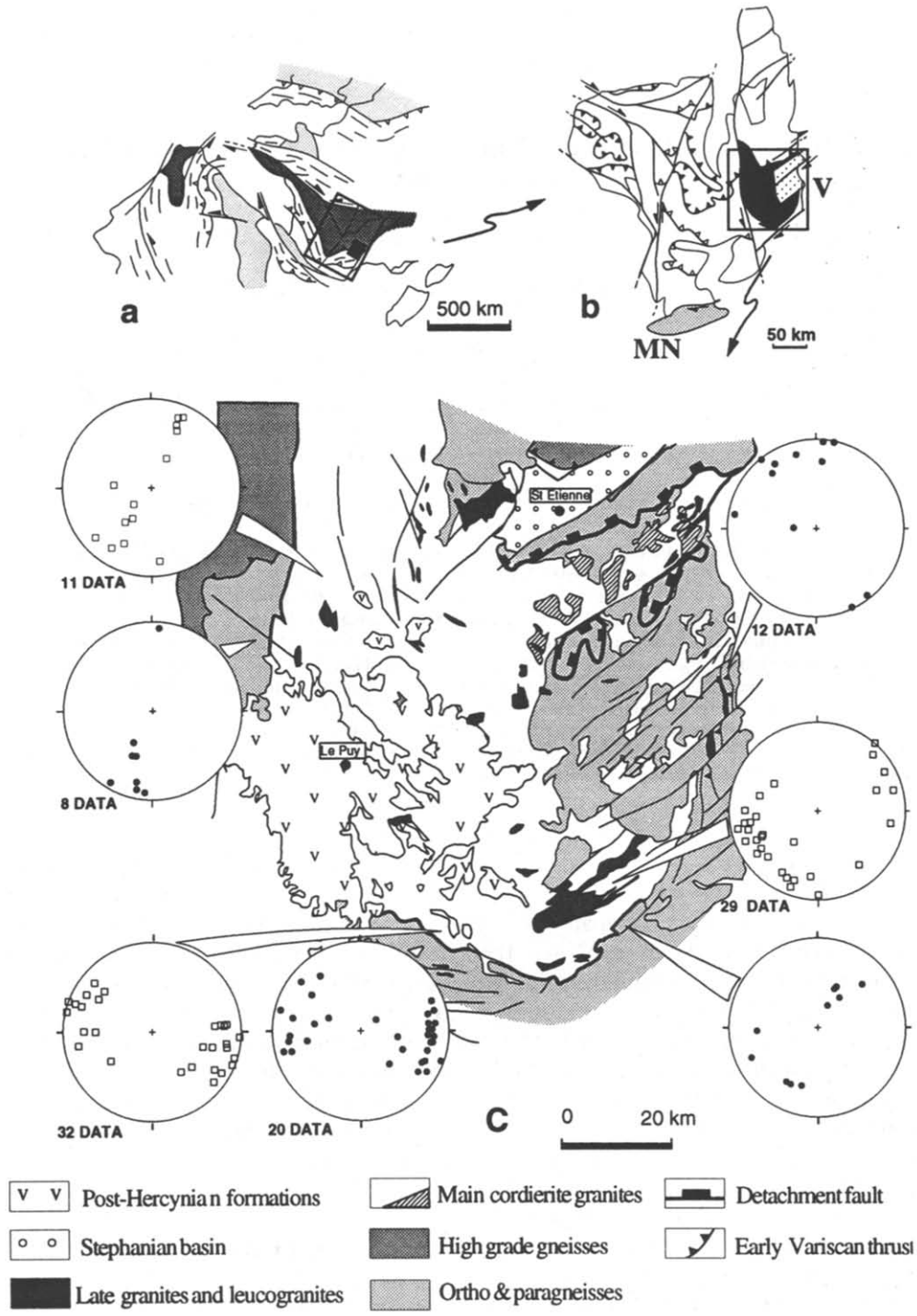

Fig. 1. The Velay granite. (a) Location in the context of the Hercynian orogeny (dark grey, internides; dashed, externides; light grey, forelands) (from Choukroune *et al.* 1990). (b) Location in the context of the French Massif Central, late Variscan domes: V, Velay; MN, Montagne Noire. (c) Velay dome. Stereograms show the orientation of folds developed during granite emplacement (squares: internal fold axes; filled circles: F_3 fold axes within the basement) (lower-hemisphere, equal-area projection).

minous cordierite-bearing granites (Dupraz & Didier 1988) whose accumulation forms a hectokilometric granitic body (Fig. 1). Small intrusions of mafic diorites accompany the peraluminous crustal melts. They suggest some mantle participation and, consequently, a heat input able to amplify crustal anatexis. Late leucogranite dykes post-date the cordierite granites. Numerous slabs of the roof and the peripheral basement are preserved within the Velay granite forming kilometric enclaves. The shape of the Velay granite can be approximated by a N–S map-scale ellipse with a low aspect ratio (100/82 km). However, the northern extension of the granites, under the high-grade gneisses remains unknown. Geophysical data (Bayer & Hirn 1987) suggest a 10 km vertical thickness for the whole of the composite granitic body, indicating a sheet-like shape. On map-scale, the granitic body shows an asymmetric dome shape with: (i) a flat roof (eastern Velay); (ii) a northeast

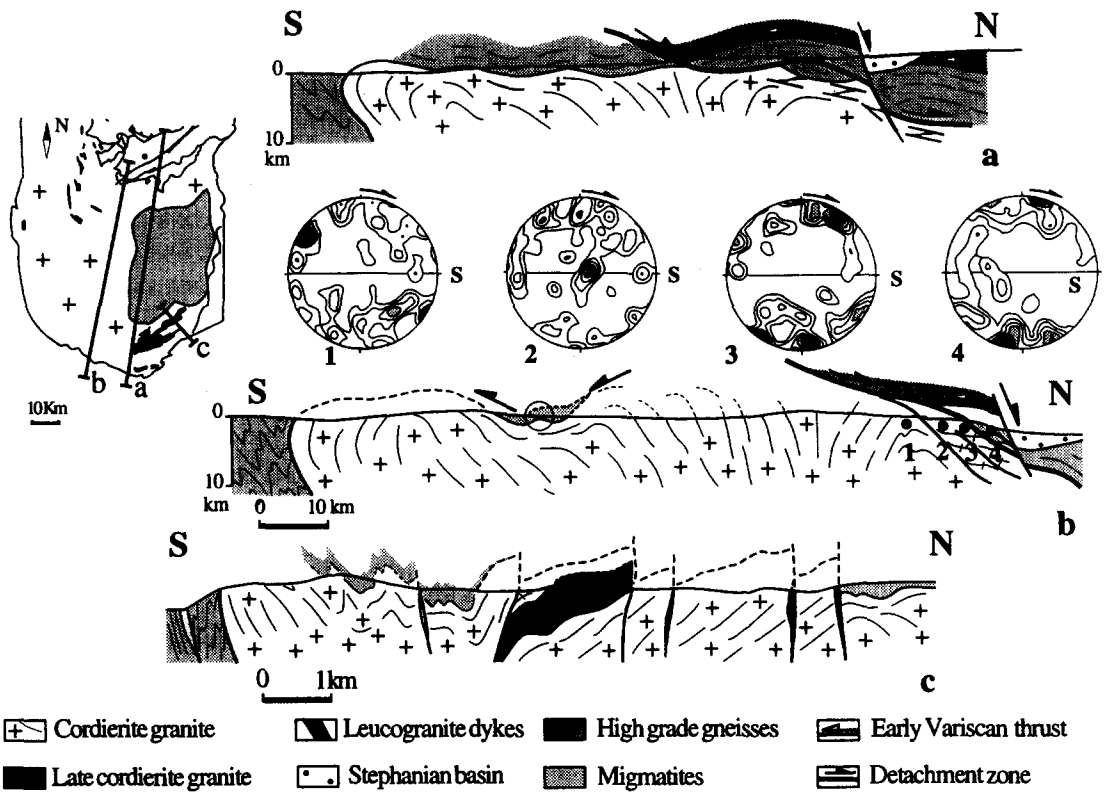

Fig. 2. Vertical cross-sections illustrating the shape of the granitic dome of the Velay. Stereograms: evolution of quartz ⟨c⟩ axes distribution ($\lambda_1\lambda_3$ plane) accompanying microstructural changes towards the Mont Pilat detachment (200 measurements per diagram, 1, 1.5, 2, 2.5 and 3 times uniform distribution).

interface gently sloping outward; and (iii) steep sides, locally dipping inward (southern Velay) as shown in Fig. 2.

Velay granites display characteristics of collision-related granitoids that are emplaced after lithospheric thickening (Lagarde *et al.* 1992). They were produced by partial melting of mid-crustal levels, during an episode of heating which followed the early thickening history (Clemens & Vielzeuf 1987, Gardien 1990, Montel *et al.* 1992). *P–T* fields related to crustal anatexis indicate a metamorphic history involving (Montel *et al.* 1992): (i) a widespread, high-temperature migmatization under water-saturated conditions (5–7 kbar, 700–750°C); (ii) granite genesis under vapour-absent, medium-pressure, high-temperature conditions (P = 5 kbar, T = 800°C); (iii) retrograde low-pressure, low-temperature conditions. This *P–T* path is consistent with the post-collisional uplift and denudation of a thickened crust. The denudation of the lower crust during the late Carboniferous is also indicated by major detachment zones which mark the northeast contact (Mattauer *et al.* 1988, Malavielle *et al.* 1990) and by Stephanian basins lying unconformably on the Variscan basement (Fig. 2).

STRUCTURES

The syn-emplacement deformation of shallow crustal granites mainly results from a continuum between high-temperature deformation processes, whether it be pre-full-crystallization processes (Hutton 1988, Paterson *et al.* 1989) or solid-state processes (Hutton 1988, Gapais 1989), and low-temperature processes (Evans 1988, Gapais 1989). Both operate during thermal re-equilibration with the lower grade host rocks. Microstructural variations record this change in deformation processes during granite cooling.

Where high-temperature processes predominate they lead to a relatively homogeneous strain, Gapais 1987, Hutton 1988, Paterson *et al.* 1989) and the granite appears often weakly deformed at the meso-scale. Homogeneous foliations (Gapais & Barbarin 1986) are frequently observed where regional effects are weak or do not significantly outlast the high-temperature deformation of the cooling granite. A controversy exists in the interpretation of such high-temperature fabrics. Although this type of fabric is sometimes ascribed to a magmatic state deformation (Blumenfeld & Bouchez 1988, Paterson *et al.* 1989), many authors pointed out that similar fabrics can be observed in metamorphic rocks where no magmatic phase has existed (Berger & Pitcher 1970, Ramsay 1989). In the same point of view, Gapais & Barbarin (1986), arguing on the basis of a detailed analysis of microscale processes conclude that homogeneous foliations were developed during high-temperature, solid-state deformation, i.e. that the possible amount of melt present does not exceed the critical melt percentage (Arzi 1978, Van der Molen & Paterson 1979).

In many cases, the tectonic setting and/or the strength contrast between granite and wall-rocks impose boundary conditions with high shear strain rates. It is the case,

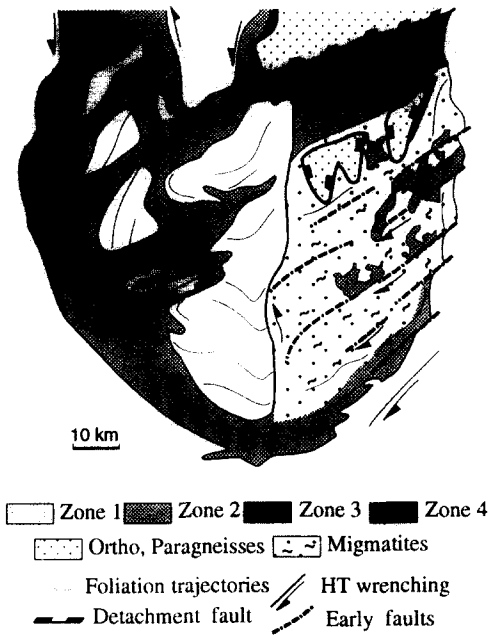

Fig. 3. Map-scale distribution of the internal strain. Strain localization is mainly linked to the temperature drop at the interface with host rocks and to ductile extensional shearing along the Pilat detachment fault.

for example, where shallow crustal granites are emplaced along ductile transcurrent or normal faults (Berthé *et al.* 1979, Hutton 1982, Burg *et al.* 1984). If enduring long enough, these boundary conditions are able to promote the widespread development of high- to moderate-temperature processes, leading to heterogeneous deformations within granites. Pervasive foliations and ductile shear bands (e.g. *S–C* structures) are observed. They facilitate the geometric and kinematic analysis of the internal deformation (Berthé *et al.* 1979, Simpson & Schmid 1983) and they give good indications on the mechanical and thermal history of the cooling granite.

Foliation development

The foliation is a planar structure defined by the preferred orientation of crystals, xenoliths and enclaves. It is due to deformation, whatever the origin of this deformation: internal buoyancy forces solely or in combination with regional tectonics (Hutton 1988, Ramsay 1989). Thereby we consider that foliation within granites is oriented perpendicular to the direction of maximum finite shortening (λ_3) (Burg *et al.* 1984, Hutton 1988, Ramsay 1989). The linear mineral alignment, observed on the foliation surface, defines the stretching lineation. This lineation, marked by elongate quartz and mica aggregates, indicates the direction of the major axis (λ_1) of the finite strain ellipsoid.

Within the Velay granite the foliation is not homogeneously distributed. Weakly foliated granites crop out in the core of the intrusion, whereas strongly foliated granites are located near the boundary with the host rocks (Fig. 3). Four zones are recognized on the basis of the progressive foliation development.

(1) *Zone 1* refers to a slightly deformed granite with no obvious textural heterogeneities (Fig. 4a). Microstructural changes occur only in the development of a weak foliation, defined by a slight planar to planar-linear orientation of feldspar porphyroblasts and micas, without plastic deformation. At the microscale, quartz grains of the matrix do not show any crystallographic preferred orientation, which therefore implies a highly ductile matrix and a high-temperature deformation (Gapais 1987).

(2) *Zone 2* refers to a deformed granite showing a homogeneous foliation (Fig. 4b), which bears a weak stretching lineation. The homogeneous foliation is defined by a planar preferred orientation of feldspars and micas, and is locally accentuated by prismatic sillimanite. Microstructural changes involve the development of shape-preferred orientations accompanied by a moderate internal deformation of crystals. Quartz grains are slightly elongated, and have lobate shapes (Fig. 4d). Lobate shapes indicate a high mobility of quartz grain boundaries and a high temperature of deformation (Lister & Dorsiepen 1982, Gapais & Barbarin 1986). Quartz $\langle c \rangle$ axes tend to concentrate close to λ_1 (1 in Fig. 2), suggesting high-temperature prism $\langle c \rangle$ slip (Blacic 1975, Schmid *et al.* 1981, Schmid & Casey 1986).

In this second zone of the microstructural history, the migration of quartz grain boundaries indicates that migration-recrystallization processes were still active and implies a high-temperature solid-state deformation (Gapais & Barbarin 1986).

(3) *Zone 3* refers to a strongly foliated granite, characterized by the association of a homogeneous foliation with small-scale shear bands (Fig. 4c). Shear bands are marked by the curvature of the foliation (*S* surfaces) along shear planes (*C* surfaces) leading to sigmoidal *S–C* structures (Berthé *et al.* 1979). Within zone 3, shear bands are weakly amplified and coexist with preserved high-temperature microstructures. At the microscale, microstructural changes include the generalization of intracrystalline strain features indicating a pervasive solid-state deformation, but under high-temperature conditions. Although feldspar grains are fractured: (i) crystallization of quartz filled these fractures (Fig. 4e); and (ii) quartz grains within the matrix locally display undulatory extinction, but myrmekite development and extensive lobate or mosaic-like patterns of quartz grains indicate that grain boundary migration and diffusion processes were still active. Quartz $\langle c \rangle$ axes display a complex pattern: the concentration close to λ_1, inherited from the high-temperature preferred orientation, disappears progressively and a maximum concentration develops close to λ_2, indicating the activation of $\langle a \rangle$ slip (2 in Fig. 2). This pattern reflects a transition from high-temperature prism $\langle c \rangle$ slip to medium-temperature $\langle a \rangle$ slip.

In the Velay granite, the development of strongly foliated granites marks an increase in strain localization and corresponds to a transition from high-temperature to medium-temperature fabrics. The development of

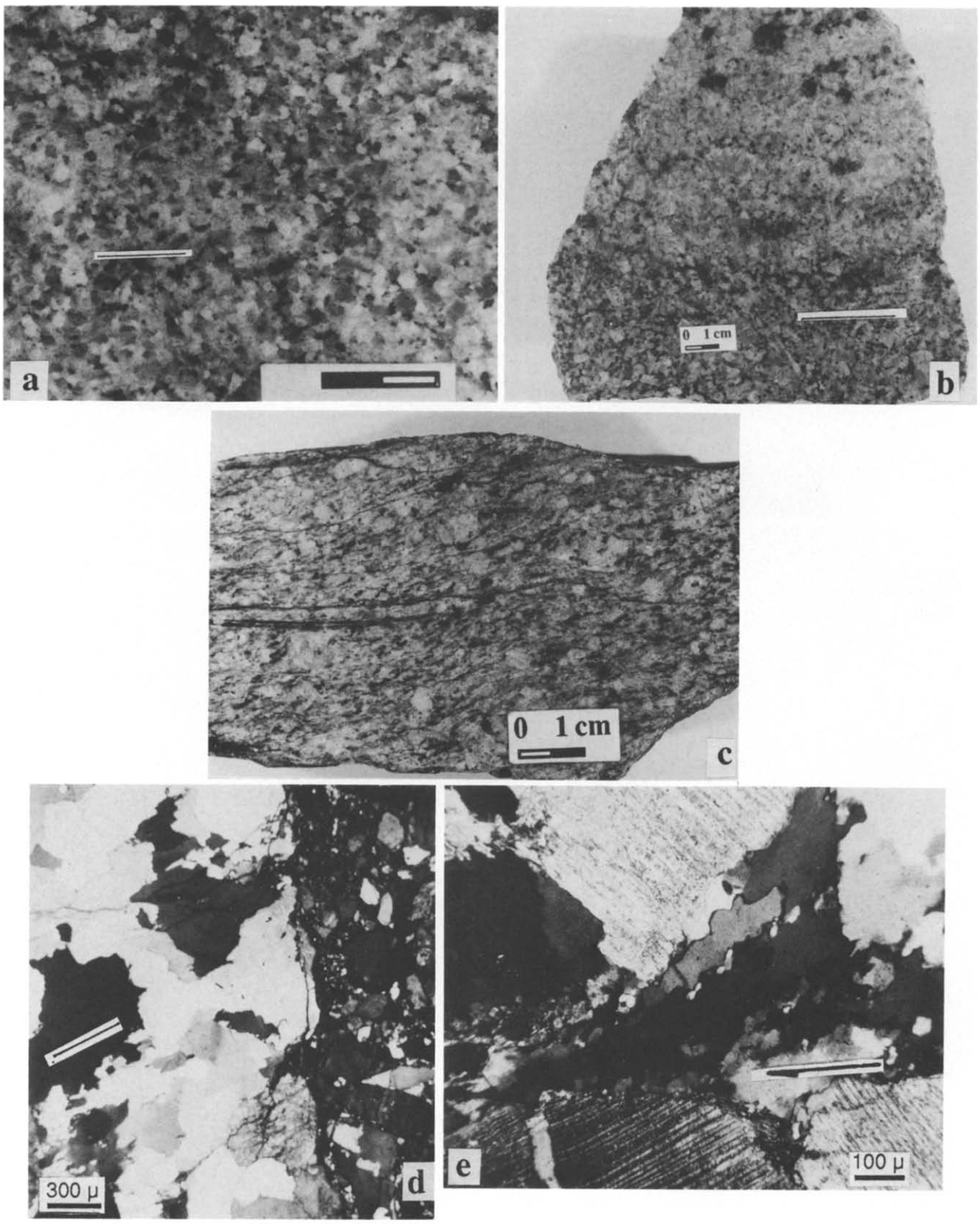

Fig. 4. Granite deformation. (a) Weak foliation (indicated) marked by slight planar to planar-linear orientation of feldspars and micas (zone 1). (b) High-temperature homogeneous foliation (zone 2). (c) Shear bands within a strongly foliated granite near the roof of the dome (zone 4). (d) Homogeneous foliation (underlined) cross-cutted by cataclasites. Lobate quartz grain boundaries indicate migration-recrystallization processes and suggest high-temperature solid-state deformation (zones 2 and 3). (e) Shear bands (arrowed) mark the strain localization at the microscale (zone 4). (d) & (e) Photomicrographs with nicols crossed.

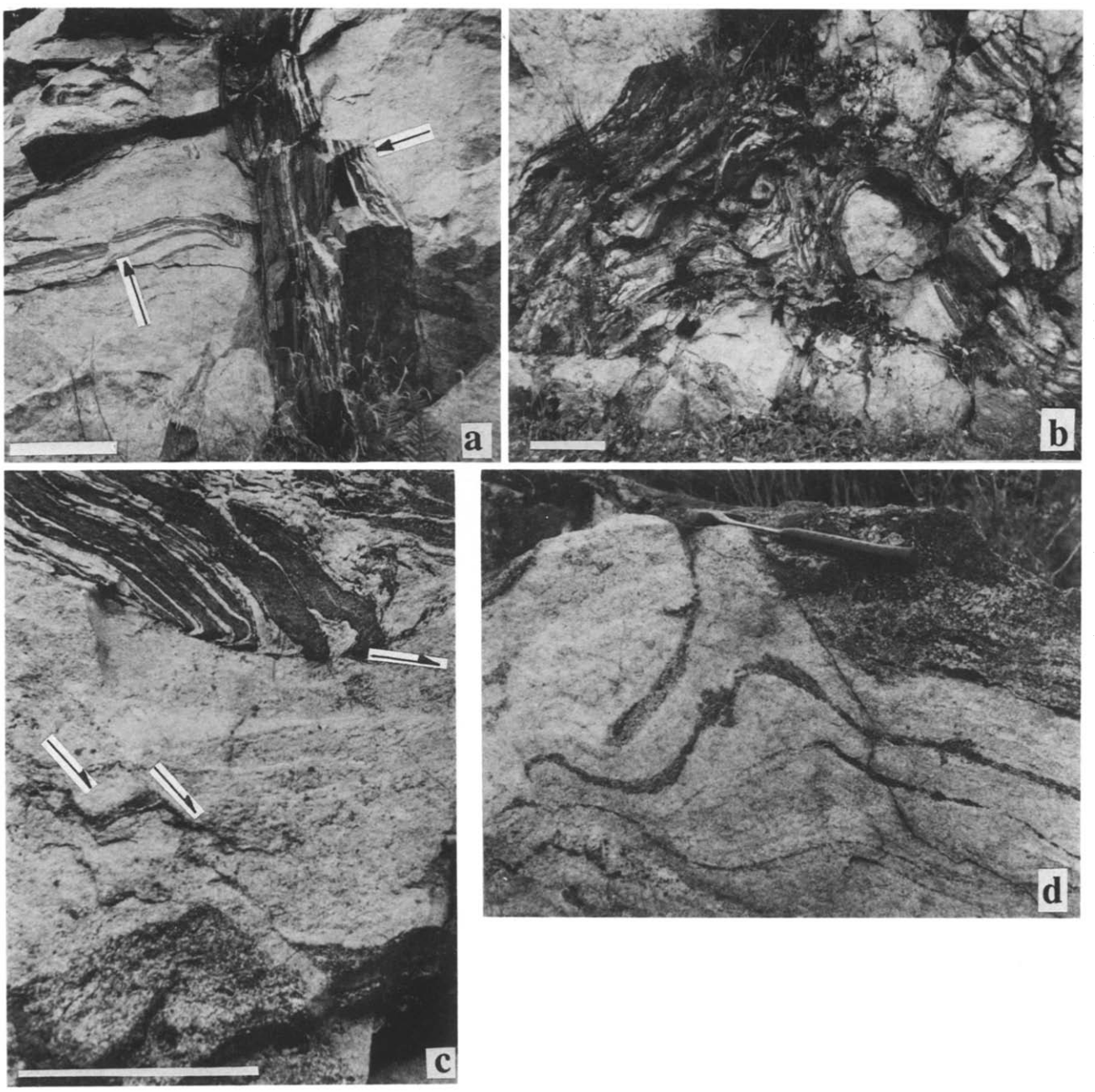

Fig. 5. (a) Mafic dykes emplaced within conjugate sets of primary joints (arrowed) developed during the hardening of the magma. (b) Folding of early mafic dykes during the lateral expansion of granites. (c) Southward extensional shears and high-temperature small-scale normal faults. (d) Horizontal shortening and folding of biotitic layers. (Scale bars: 0.3 m.)

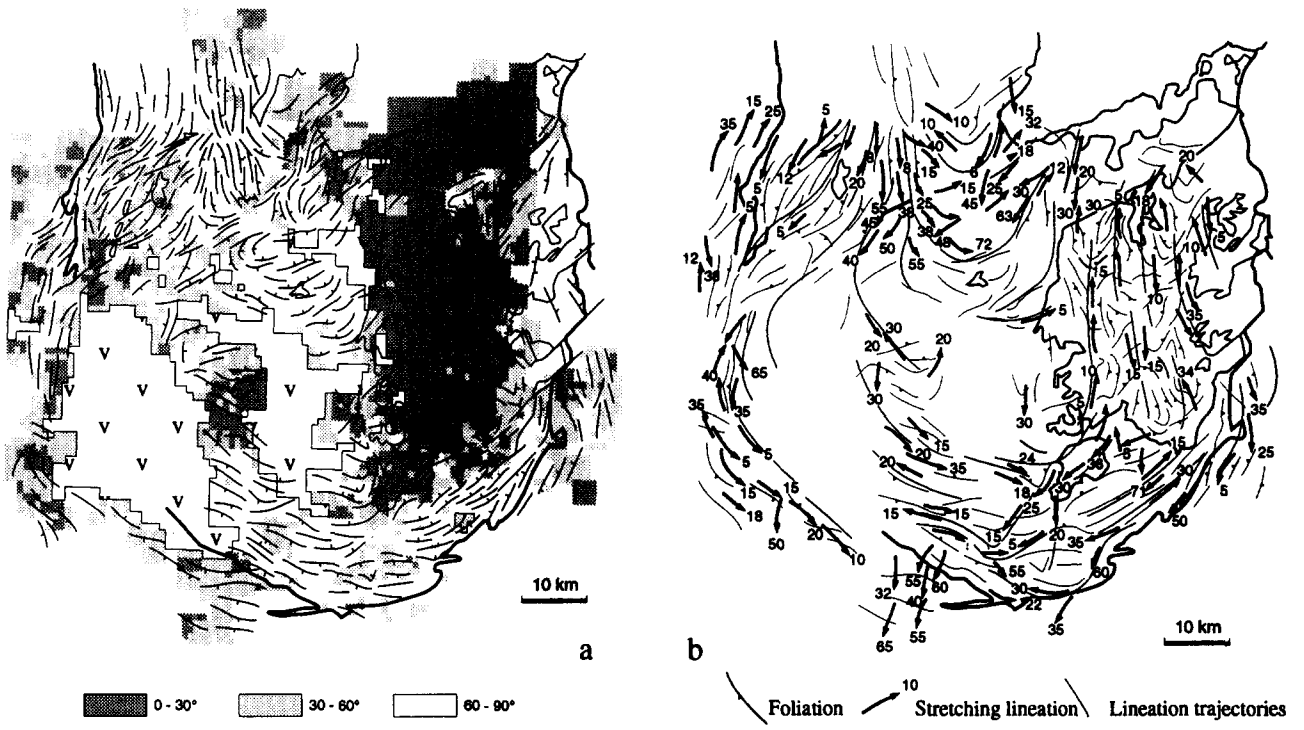

Fig. 6. (a) Map-scale foliation trajectories showing concentric patterns in central and southern Velay. Flat lying foliations are located at the top of the dome (eastern Velay). (b) Stretching lineation shows a concentric pattern except at the rear, on the flanks and near the top of the dome where N–S stretching is parallel to the main direction of extension (about 5000 data points are summarized; curved stretching lineation symbols result from the integration of several data points).

the foliation is favoured, at the grain scale, by the efficiency of softening processes, such as migration-recrystallization at high temperatures, then rotation-recrystallization at lower temperatures (Guillopé & Poirier 1979, Gapais & Barbarin 1986). These deformation mechanisms tend to weaken the granite and to localize the deformation.

(4) *Zone 4* refers to *S–C* orthogneisses (Berthé *et al.* 1979). In this zone, the homogeneous foliation undergoes a heterogeneous shear strain characterized by the amplification and propagation of the weak shear bands previously formed (Fig. 4c). Strain gradients are developed on the microscale. This results in grain-size reduction along shear bands accompanied by a prominent internal deformation. Quartz ⟨*c*⟩ axes tend to plot within asymmetric crossed girdles (3 in Fig. 2). This kind of preferred orientation reflects a dominant (0001) basal slip, which developed at medium to low temperature (below 550°C) (Lister & Williams 1979, Bouchez & Pêcher 1981, Gapais 1987, 1989). In this zone the amplification of shear bands marks the strain localization at the microscale, and the evolution from solid-state stable deformation to localized unstable deformation.

In the Velay granite, the foliation is locally cross-cut by cataclasites that have developed along discrete shear planes (Fig. 4d). Cataclastic deformation induced a strong grain-size reduction in the quartz and feldspars, whereas micas were altered and then disappeared. This cataclastic process characterizes brittle shallow crustal conditions (Sibson 1977, Evans 1988) within early fault zones.

The continuum between weak homogeneous foliations, high- to medium-temperature heterogeneous shear bands and low-temperature cataclasites reflects a decrease in the temperature of deformation linked to the cooling history of the Velay granite. This retrograde evolution of the internal deformation, from the inner to the outer parts of the granite, is diagnostic of foliation development during granite emplacement (Hutton 1988, Gapais 1989, Lagarde *et al.* 1990a).

Folds and early faults

Folds are well developed near the southern contact, in zones of flat-lying foliation and flat-lying lithological heterogeneities. They consist of metric to decametric upright, open and gently-plunging folds. Internal folds are initiated where viscosity contrasts exist (Stel 1991) as, for instance, near biotite schlierens, basement slabs or along early mafic dykes (Fig. 5).

The progressive development of primary joints and early faults relates to a syn-emplacement brittle deformation and reflects the hardening of the magma, due to cooling. Joints and early faults display complex patterns and channel the emplacement of late melts giving rise to mafic diorite dykes (Fig. 5) or late cordierite granite pods (Dupraz & Didier 1988).

STRAIN PATTERNS

Finite strain trajectories

Maps of finite strain trajectories (flattening plane and λ_1 orientations) are presented in Fig. 6. They take into account more than 5000 measurements of foliation and stretching lineation in the granitic dome of the Velay. Finite strain trajectories are characterized by: (i) map

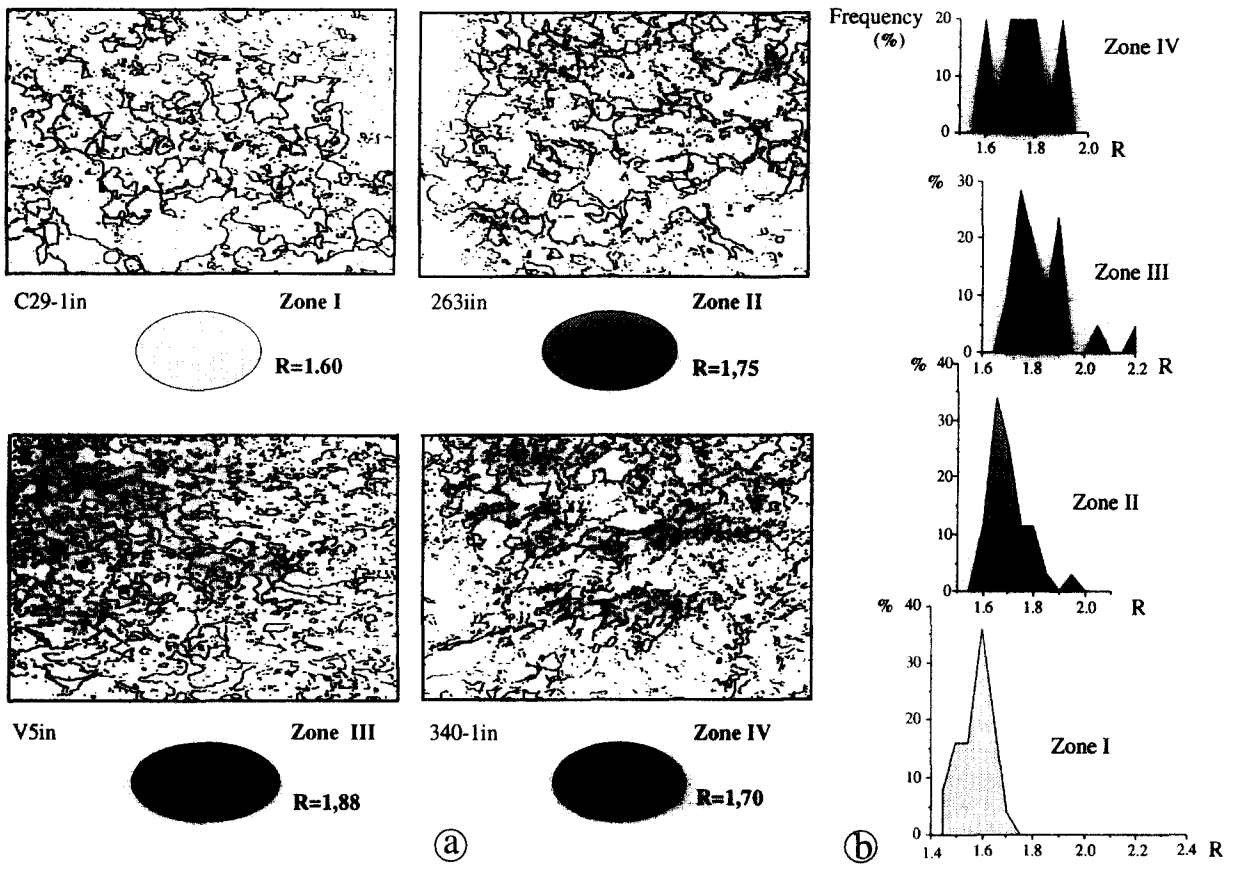

Fig. 7. (a) Digitization by image processing of grain boundary outlines (thin sections from zones I–IV, $\lambda_1\lambda_3$ planes). Ellipses show variations of the relative strain state, estimated using the inverse SURFOR wheel method which takes into account the probability of grain boundaries being intersected on given traverses (Pannozo 1987) (R = axial ratio of the strain ellipse). (b) Diagrams show, in each zone, the distribution of R parameter values (number of image processed from zones I–IV: 25, 35, 21 and 5).

scale concentric patterns of the foliation which is parallel to the external boundary of the dome; (ii) steeply dipping foliations (western Velay) becoming sub-horizontal near the top (eastern Velay); (iii) concentric stretching lineations in central and southern Velay; (iv) N–S stretching lineations on the flanks, at the top of granites and within overlying host rocks; (v) folding of the foliation, of the basement slabs and of the early dykes where they are flat-lying, i.e. near the top of granites (Fig. 2); and (vi) concentric pattern of the internal folds (Fig. 1).

Strain-state variations

The lack of reliable strain markers in the Velay granite prevents a precise analysis of the finite strain ellipsoid. Strain-state variations and strain intensity patterns have been estimated using an original method of fabric analysis: the inverse surfor wheel (Pannozo 1987). This method gives an estimation of the strain recorded in the preferred orientation of grain boundaries (i.e. lines). It takes into account the probability of grain boundaries being intersected on given traverses.

In the Velay granite, grain boundary surfaces do not act exclusively as passive markers because of the existence of dynamic recrystallization and grain boundary migration. Therefore, the fabric analysis does not relate exactly to the finite strain ellipsoid. Only relative strain state variations are inferred. In our analysis, grain boundary outlines were digitized by image processing and the inverse surfor wheel was obtained by a computer-based method (Niorthe 1990). This treatment was applied to the different zones of deformation inferred from the qualitative evolution of microstructures. More than 80 images were treated and the results are presented in Fig. 7. Strain intensity profiles in the ($\lambda_1\lambda_3$) principal plane show an increase from zone 1 to zones 3 and 4. A strain decrease is observed between zone 3 and zone 4, probably because of the strong dynamic recrystallization and the local misorientation induced by shear bands. These results give a good idea on strain variations and on strain intensity patterns in the Velay granite. They are consistent with strain variations suggested by the microstructural evolution.

Localization of deformation

The localization of deformation in the Velay granite results mainly from thermal and structural heterogeneities.

Thermal heterogeneities are linked to the decrease in temperature during thermal re-equilibration of granites. They give rise to strain concentration in marginal zones, i.e. in zones where the temperature drop is expected to

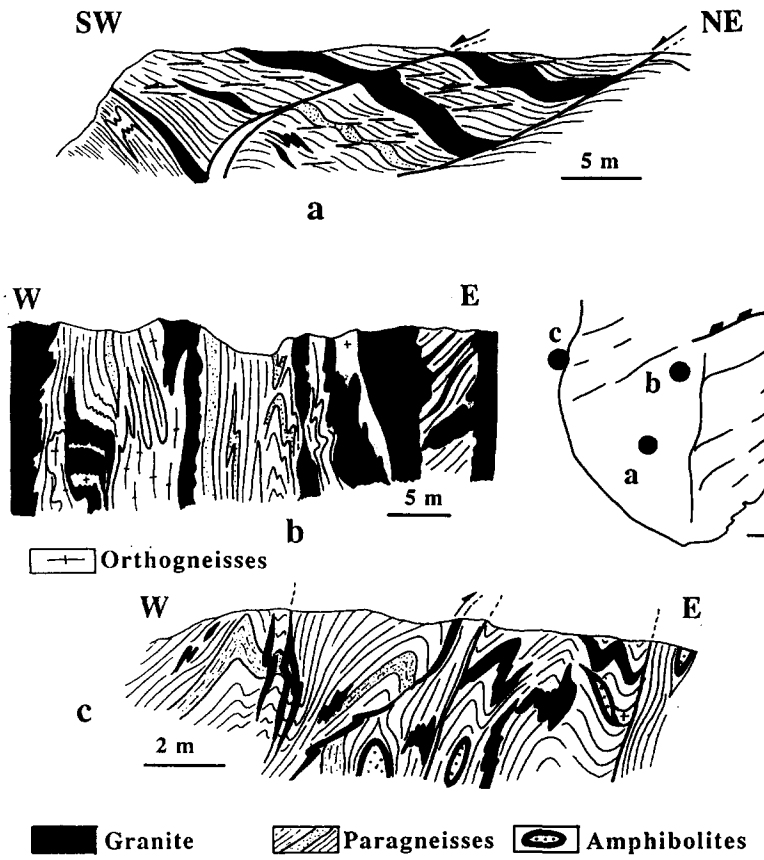

Fig. 8. (a) Top-to-the-south extensional shears observed within basement slabs near the top of the dome. (b) Steeply dipping enclaves of paragneisses and orthogneisses. (c) Deformation in peripheral wall rocks related to granite emplacement: the flat-lying regional foliation S_{1-2}, inherited from the thickening episode, is deformed by gently plunging F_3 folds which are parallel to the external boundary of the dome (see stereograms, Fig. 1c).

be rapid. This pattern, which relates to the cooling history, reflects also the strength contrast between granites and wall-rocks during magma emplacement.

Structural heterogeneities have an influence on the evolution of the internal deformation. A localized deformation develops where a high imposed shear strain rate prevents the granite from accommodating the imposed boundary displacements in a homogeneous way. This is the case: (i) where the Mont Pilat detachment zone bounds the granitic dome; (ii) where ductile shear zones develop along contacts and within granites; and (iii) where granites include large lithological heterogeneities, such as hectometric basement slabs (Fig. 3).

Granite emplacement and doming control the microstructural evolution and the localization of deformation in wall-rocks. Indeed, the emplacement of a large volume of hot granitic magma in the middle to upper crust induces thermal and mechanical instabilities. It gives rise to a thermal softening and favours strain localization within the peripheral host rocks (Hutton 1988, Lagarde *et al.* 1990a). Perturbations of the regional strain pattern, that we relate to granite emplacement, consist of the development of superimposed structures associated with changes in finite strain trajectories. The flat-lying regional foliation S_{1-2} inherited from the thickening episode, is deformed by gently plunging F_3 folds with S_3 axial plane cleavage (Fig. 8). The correspondance between D_3 deformation and granite emplacement is supported by a three-fold argumentation: (i) on the flanks of the granitic dome S_{1-2}, S_3 foliations and F_3 fold axes tend to become conformable to the granite interface and show a concentric pattern (Fig. 1); (ii) meso-scale layers of granitic melts pre-date and post-date F_3 folds (Fig. 8); and (iii) S_3 foliation is marked by high-temperature assemblages (Gardien 1990) developed during the high-temperature event which accompanies granite emplacement (Montel *et al.* 1992).

Kinematics of deformation

A variety of shear sense indicators can be recognized in deformed granites of the Velay dome (zones 3 and 4, Fig. 3): foliation curvature and re-orientation of lithological heterogeneities (Ramsay & Graham 1970); asymmetric *S–C* fabrics (Choukroune *et al.* 1987); asymmetric quartz ⟨*c*⟩ axis distributions (Simpson & Schmid 1983) and rolling structures (Passchier & Simpson 1986). They relate to a combination of extensional shearing and wrenching.

Extensional shears are dominant near the roof of the dome. In northern Velay they are best developed along the Mont Pilat detachment fault (Malavielle *et al.* 1990)

(Fig. 2) where oblique top-to-the-north displacements indicate a combination of dominant dip-slip and dextral strike-slip displacements. They are associated to medium- to low-temperature heterogeneous deformation marked by the development of amplified *S–C* shear bands, locally overprinted by cataclasites and they suggest boundary conditions with a high imposed shear strain rate. In southern Velay, meso-scale extensional shear zones indicate top-to-the-south displacements and are associated with high-temperature southward-sloping normal faults, boudinage of the magmatic layering and rolling structures (Fig. 5). These two zones showing opposite displacements are separated by a zone with conjugate sets of extensional shears.

Ductile wrench components can be detected: (i) near the western contact with wall-rocks where strongly foliated granites and *S–C* orthogneisses indicate sinistral displacements; and (ii) within localized internal wrench zones that occur in conjugate sets with N–S sinistral and ENE–WSW dextral displacements (Lagarde *et al.* 1990c) (Fig. 6). Internal wrench zones are characterized by homogeneous foliations associated to weakly amplified shear bands which indicate the predominance of high-temperature deformation processes. They show the same orientation and kinematics as late Variscan shear zones described within host rocks (Ledru *et al.* 1989).

In this kinematic pattern, extensional shears and dip-slip components reflect a prominent horizontal N–S to NNE–SSW extension during granite emplacement whereas ductile wrench zones indicate localized strike-slip component. This kinematic pattern is quite similar to that described in the neighbouring dome of the Montagne Noire where NE–SW extensional shearing is combined with N–S sinistral and ENE–WSW dextral wrenching (Echtler & Malavieille 1990).

INTERPRETATIONS

Strain components and kinematics of granite emplacement

According to strain components, two zones can be distinguished in the Velay dome.

(1) In central and southern Velay, the characteristics of the internal deformation support the hypothesis that granites were emplaced with a dominant component of lateral expansion. Indeed, concentric patterns (foliations, stretching, folds) and steeply dipping foliations relate to a horizontal radial shortening as expected when granite expands laterally at the site of final emplacement (Brun *et al.* 1990). Foliation curvatures towards the top (Fig. 2) reflect divergent shear against flat roof, consistent with a component of vertical shortening. Similar patterns are expected when gravity collapse interferes in the strain field as shown by modelling of extruding-spreading nappes (Merle 1989). In the Velay, these patterns suggest a southward expansion also indicated by the top-to-the-south extensional shears described above. This lateral expansion was probably facilitated by temperatures during the emplacement of granites which were high enough to enhance the weakening of the peripheral basement (Montel *et al.* 1992). In the same point of view southward-directed overturned folds with inverted limbs, recognized in southern wall-rocks (Burg & Vanderhaeghe 1993), indicate frontal rolling effects that also relate to a southward spreading of the Velay granitic dome. However the lateral expansion of the Velay granite must not be considered as evidence for a given mode of magma ascent because: (i) granite expansion may be the consequence of both diapirism, *in situ* assemblage of laterally expanding magmas (Lagarde *et al.* 1990c, Brun *et al.* 1990), gravity collapse (Merle 1989) or extensional tectonics (Lister & Davis 1989); (ii) most of the internal microstructures relate to the development of a solid-state deformation; and (iii) expansion-controlled foliations are concentric and peripheral stretching lineations are shallow plunging; they cannot be related to the history of magma ascent which is expected to involve widespread vertical movements. The lateral expansion of the Velay granite merely reflects the geometry and kinematics of granite deformation, at the site of final emplacement.

(2) In northern Velay the lateral expansion is restricted and combined with regional effects such as top-to-the-north extensional shearing and high-temperature wrenching. Both accommodate horizontal N–S extension.

This strain pattern within the Velay granites results in a strongly asymmetric dome whose northern part suffered a northward extensional shear combined with wrenching whereas central and southern parts suffered southward spreading (Fig. 9).

Tectonic setting of granite emplacement

Many authors have previously shown that the geometry and kinematics of granite deformation deduced from analysis of strain patterns provide good indications on the tectonic environment during final emplacement of granites (Brun & Pons 1981, Hutton 1982, 1988, Castro 1987, Courrioux 1987, Lagarde *et al.* 1990a).

Strain patterns in the granitic dome of the Velay can be compared with those expected when granite emplacement coincides with wrench or thrust tectonics and with extensional tectonics.

(1) Field data and numerical modelling have led to a detailed description of strain patterns related to the interference between granite emplacement and regional deformation (Brun & Pons 1981, Hutton 1988). Granites emplaced during regional wrenching have typical strain patterns with sigmoidal or helicoidal foliation trends and slightly plunging stretching lineations. The internal foliation shows a geometrical continuity with the foliation in wall-rocks and foliation triple-points are observed at the extremities of granites (Figs. 10a & b). On the other hand, granites emplaced during regional thrusting show eccentric foliation patterns and down-dip stretching lineations. Foliation triple-points develop lat-

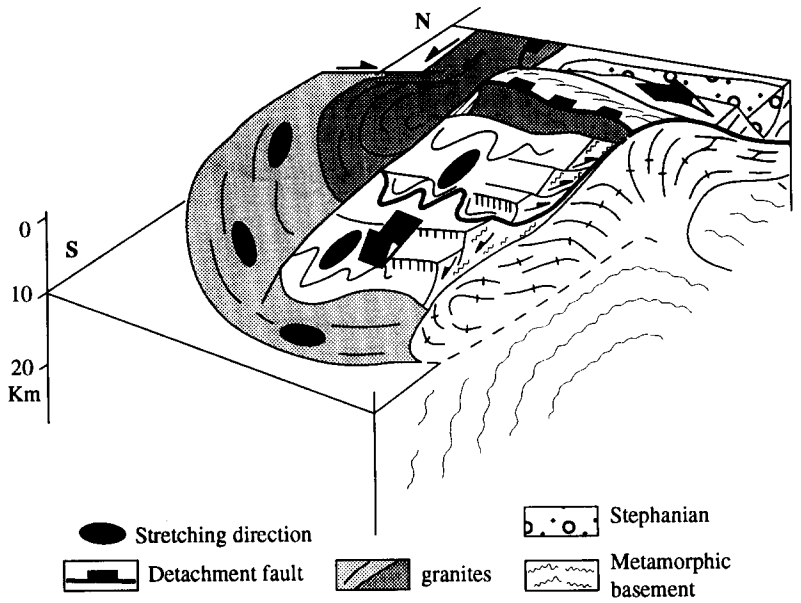

Fig. 9. Three-dimensional sketch showing the asymmetrical pattern of deformation within the granitic dome of the Velay: central and frontal parts, characterized by concentric patterns, suffered southward spreading whereas the northern part suffered northward extensional shearing along the Mont Pilat detachment.

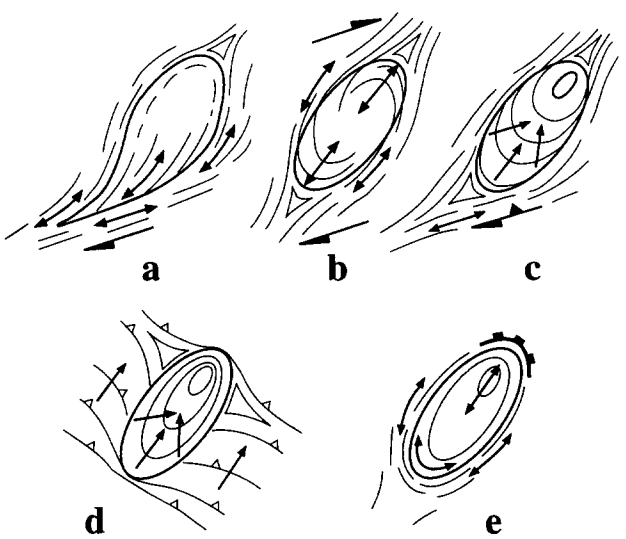

Fig. 10. Tectonic setting of granite emplacement and related strain patterns. (a) Emplacement along a strike-slip fault. (b) Regional wrenching. (c) Thrust-wrench shear zone. (d) Regional thrusting. (e) Laterally expanding and spreading granites emplaced below a detachment fault. Foliation trajectories (lines), stretching lineation (arrows). (b) & (d) from Brun & Pons (1981).

erally (Fig. 10d). Deformation in the dome of the Velay cannot be clearly related to the former pattern, i.e. to extensive regional wrenching. Nevertheless, as stated before, wrenching is one of the internal strain components and late Carboniferous regional wrench zones have been described in wall rocks as, for example, along the western contact (Burg *et al.* 1990, Lagarde *et al.* 1990c). Otherwise strain patterns in southern Velay could be partly explained by syn-emplacement thrusting along an active south vergent thrust close to the present roof contact, giving flat fabrics and N–S lineations. Although a similar interpretation has been recently presented (Ledru *et al.* 1991), this hypothesis does not fully explain the deformation pattern and, in particular, it does not account for the top-to-the-north extensional shearing.

(2) Strain patterns in the dome of the Velay show many similarities with those expected when doming occurs during extensional tectonics (Davis 1983, Coney & Harms 1984, Wernicke & Burchfield 1982, Lister & Davis 1989, Echtler & Malavieille 1990, Carmignani & Kligfield 1990, Hill *et al.* 1992, Van Den Driessche & Brun 1992). These similarities include: (i) the occurrence of a major detachment zone that bounds one side of the dome; (ii) the record of extensional shearing in the internal strain pattern which attests to the coincidence between doming and detachment; (iii) the evolution from ductile to cataclastic processes; and (iv) the global asymmetry of the dome. Despite these similarities, the dome of the Velay shows certain unique features which have to be explained. A peculiarity is the occurrence of southward displacements, in an opposite sense to extensional shears along the detachment zone. These divergent displacements can be related both to: (i) doming effects (Dixon 1975); (ii) gravity collapse (Merle 1989); and (iii) tectonic effects linked to a regional southward décollement of the southern overlying unit (Fig. 11). Divergent displacements in the Velay fit well with deformation patterns predicted in numerical modelling of the isostatic rebound of the lower crust due to tectonic denudation (Spencer 1984, Wdowinski & Axen 1992). Following these models the tectonic denudation of the upper crust, by detachment faults, results in a curvature and a doming of the footwall which flows toward the detachment. Because of the footwall curvature the ramp of the detachment is progressively rotated and becomes flat-lying. This process results in a convex geometry of the detachment at the top of the uplifted lower crust and divergent simple shear components are expected on the sides of the footwall dome (Malavieille & Taboada 1991, Wdowinski & Axen 1992). Another originality of the

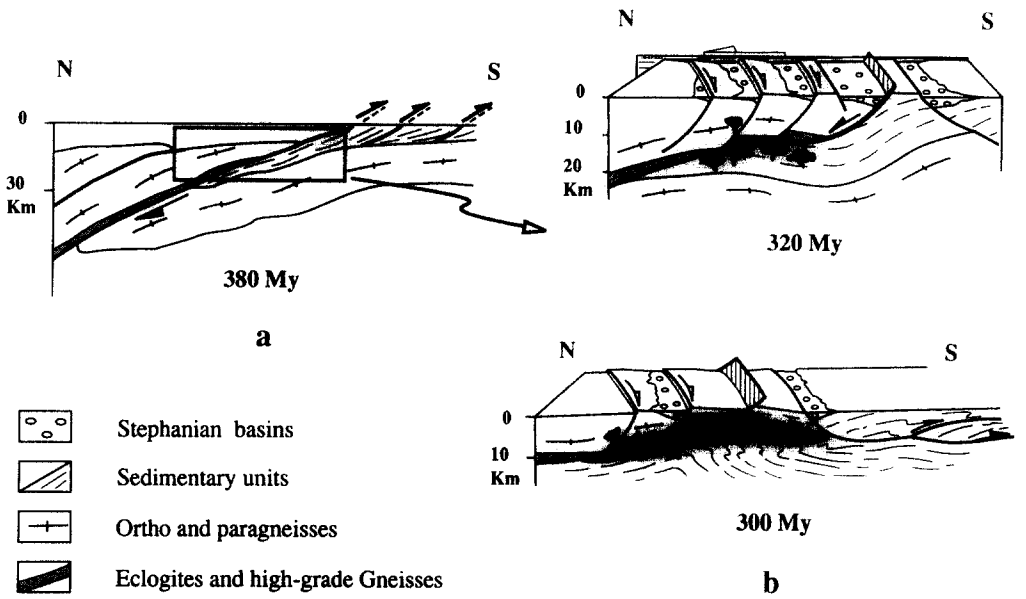

Fig. 11. Tectonic evolution proposed for the Velay area. (a) Northward underthrusting and crustal thickening during Variscan convergence. (b) Partial melting and anatectic granite production during late Variscan tectonic denudation and isostatic rebound of the lower crust. The uplifted crust is progressively invaded by a large amount of anatectic granites which emplaced below high-grade gneisses, along a detachment zone. Granites register oblique extensional shearing near the detachment and extensive southward spreading elsewhere giving rise to an asymmetrical dome. Strike-slip faults observed at the boundaries of the dome could have acted as transfer faults.

deformation pattern in the Velay granite and host rocks is the combination of extensional tectonics and wrenching. This combination suggests that the onset of extensional deformation may have coincided with late Carboniferous wrenching (Arthaud & Matte 1977). Wrench faults may also have acted as transfer faults accommodating differential displacements during the post-thickening history of the Variscan belt (Burg *et al.* 1990).

CONCLUSIONS

(1) In the late Variscan granitic dome of the Velay, strain patterns relate to the geometry and kinematics of deformation during granite emplacement and at the site of final emplacement.

(2) Strain is concentrated in marginal zones and in extensional or wrench shear zones.

(3) Microstructural changes related to foliation development involve a continuum between weak homogeneous foliations, high- to medium-temperature heterogeneous shear bands and low-temperature cataclasites. They indicate a retrograde evolution of the internal deformation linked to the cooling history of granites.

(4) Inferred strain components point out the strong asymmetry of the dome: the northern part suffered a northward extensional shearing combined with wrenching whereas central and southern parts suffered southward spreading.

The geometry and kinematics of the deformation within the granitic dome of the Velay provides some useful constraints for our understanding of late Variscan history (Fig. 11). This history can be summarized as follows.

(1) The partial melting of a crustal slab, previously underthrusted to the north during the Variscan convergence, leads to anatectic granite production during a post-thickening episode of heating.

(2) Late Variscan tectonic denudation, isostatic rebound and uplift of the lower crust occurred afterwards during N–S extension of the area, contemporary with crustal-scale wrenching. The uplifted lower crust is progressively invaded by a large amount of anatectic granites which emplaced below the detachment zone of the Mont Pilat, giving rise to an asymmetrical granitic dome. The deformation registered within granites involves northward extensional shearing, near the detachment, but also extensive southward spreading elsewhere. In this scenario, the granitic dome of the Velay can be interpreted as a post-thickening asymmetric dome developed during late Variscan combination of extensional and wrench tectonics.

Acknowledgements——The authors wish to thank J.-P. Brun, J.-P. Burg, D. Gapais and J. Van Den Driessche for helpful discussions on granitic domes. We are greatly indebted to R. J. Lisle and two anonymous referees for their helpful reviews and constructive criticism.

REFERENCES

Arthaud, F. & Matte, P. 1977. Late Paleozoic strike-slip faulting in southern Europe and northern Africa: result of right lateral shear zone between the Appalachians and the Urals. *Bull. geol. Soc. Am.* **88**, 1305–1320.

Arzi, A. A. 1978. Critical phenomena in the rheology of partially melted rocks. *Tectonophysics* **44**, 173–184.

Bayer, R. & Hirn, A. 1987. Données géophysiques sur la structure profonde de la croûte hercynienne dans l'arc ibero-armoricain et le massif central français. *Bull. Soc. géol Fr.* **3**, 561–574.

Berger, A. L. & Pitcher, W. S. 1970. Structures in granite rocks: a commentary and a critique on granite tectonics. *Proc. Geol. Ass. Lond.* **81**, 409–420.

Berthé, D., Choukroune, P. & Jegouzo, P. 1979. Orthogneiss, mylonite and non-coaxial deformation of granite: the example of the South Armorican Shear Zone. *J. Struct. Geol.* **1**, 31–42.

Blacic, J. D. 1975. Plastic deformation mechanisms in quartz: the effect of water. *Tectonophysics* **27**, 271–294.

Blumenfeld, P. & Bouchez, J. J. 1988. Shear criteria in granite and migmatite deformed in the magmatic and solid states. *J. Struct. Geol.* **4**, 361–372.

Bouchez, J.-L. & Pêcher, A. 1981. The Himalayan Main Central Thrust pile and its quartz-rich tectonites in Central Nepal. *Tectonophysics* **78**, 23–50.

Brun, J.-P. & Pons, J. 1981. Strain patterns of pluton emplacement in a crust undergoing non-coaxial deformation, Sierra Morena, Southern Spain. *J. Struct. Geol.* **3**, 219–229.

Brun, J.-P., Gapais, D., Cogne, J. P., Ledru, P. & Vigneresse, J. L. 1990. The Flamanville Granite (NW France): an unequivocal example of syntectonically expanding pluton. *Geol. J.* **25**, 271–286.

Burg, J.-P. 1983. Tectonogénèse comparée de deux segments de la chaine de collision: le Sud du Tibet (suture du Tsangpo), la chaine hercynienne en Europe (suture du massif central). Unpublished thèse d'état, University of Montpellier.

Burg, J.-P., Brun, J.-P. & Van Den Driessche, J. 1990. Le sillon Houiller du Massif Central Français: faille de transfert pendant l'amincissement crustal de la chaîne Varisque? *C.r. Acad. Sci., Paris* **311**, 147–152.

Burg, J.-P., Brunel, M., Gapais, D., Chen, G. M. & Liu, G. H. 1984. Deformation of leucogranites of the crystalline Main Central Sheet in southern Tibet (China). *J. Struct. Geol.* **6**, 535–542.

Burg, J.-P. & Vanderhaeghe, O. 1993. Structures and way up criteria in migmatites: applications to the Velay dome (French Massif Central). *J. Struct. Geol.* **15**, 1293–1301.

Caen-Vachette, M., Couturié, J. P. & Didier, J. 1982. Ages radiométriques des granites anatectiques et tardi-migmatitiques du Velay (massif central français). *C.r. Acad. Sci., Paris* **301**, 1303–1308.

Carmignani, L. & Kligfield, R. 1990. Crustal extension in the northern Apennines: the transition from compression to extension in the Alpi Apuane core complex. *Tectonics* **9**, 1275–1303.

Castro, A. 1987. On granitoids emplacement and related structures. *Geol. Rdsch.* **76**, 101–124.

Choukroune, P., Gapais, D. & Merle O. 1987. Shear criteria and structural symmetry. *J. Struct. Geol.* **9**, 525–530.

Choukroune, P., Pinet, B., Roure, F. & Cazes, M. 1990. Major Hercynian thrusts along the ECORS Pyrenees and Biscay lines. *Bull. Soc. géol. Fr.* **8**, 313–320.

Clemens, J. D. & Vielzeuf, D. 1987. Constraints on melting and magma production in the crust. *Earth Planet. Sci. Lett.* **86**, 287–306.

Coney, P. J. & Harms, T. 1984. Cordilleran metamorphic core complexes: Cenozoic extensional relics of Mesozoic compression. *Geology* **12**, 550–554.

Courrioux, G. 1987. Oblique diapirism: the Criffel granodiorite/granite zones pluton (SW Scotland). *J. Struct. Geol.* **3**, 313–330.

Davis, G. H. 1983. Shear-zone model for the origin of metamorphic core complexes. *Geology* **11**, 342–347.

Dixon, J. M. 1975. Finite strain and progressive deformation in models of diapiric structures. *Tectonophysics* **28**, 89–124.

Dupraz, J. & Didier, J. 1988. Le complexe anatectique du Velay (Massif Central Français) : Structures d'ensembles et évolution géologique. *Géol. Fr., B.R.G.M.* **4**, 73–88.

Duthou, J. L., Cantagrel, J. M., Didier, J. & Vialette, Y. 1984. Paleozoic granitoids from the French Massif Central: age and origin studied by ^{87}Rb–^{87}Sr system. *Phys. Earth & Planet. Interiors* **35**, 131–144.

Echtler, H. & Malavieille, J. 1990. Extensional tectonics, basement uplift and Stephano-Permian collapse basin in a late Variscan metamorphic core complex (Montagne Noire, Southern Massif Central). *Tectonophysics* **177**, 125–138.

Evans, J. P. 1988. Deformation mechanisms in granites rocks at shallow crustal levels. *J. Struct. Geol.* **10**, 437–444.

Gapais, D. 1987. Les orthogneiss. Structures, mécanismes de deformation et analyse cinématique. *Mem. CAESS* **28**.

Gapais, D. 1989. Shear structures within deformed granites: Mechanical and thermal indicators. *Geology* **17**, 1144–1147.

Gapais, D. & Barbarin, B. 1986. Quartz fabric transition in a cooling syntectonic granite (Hermitage massif, France). *Tectonophysics* **125**, 357–370.

Gapais, D. & Le Corre, C. 1980. Is the Hercynian belt of Britanny a major shear zone? *Nature* **288**, 574–576.

Gapais, D., Pêcher, A., Gilbert, E. & Ballèvre, M. 1992. Synconvergence spreading of the higher Himalaya crystalline in Ladakh. *Tectonics* **11**, 1045–1056.

Gardien, V. 1990. Reliques de grenat et de staurotide dans la série métamorphique de basse pression du Mont Pilat (Massif Central français): témoins s'une évolution tectonométamorphique polyphasée. *C.r. Acad. Sci., Paris* **310**, 233–240.

Guillopé, M. & Poirier, J. P. 1979. Dynamic recrystallization during creep of single-crystalline halite: an experimental study. *J. geophys. Res.* **84**, 5557–5567.

Hill, E. J., Baldwin, S. L. & Lister, G. S. 1992. Unroofing of active metamorphic core complexes in the D'Entrecasteaux Islands, Papua New Guinea. *Geology* **20**, 907–910.

Hutton, D. W. 1982. A tectonic model for the emplacement of the Main Donegal granite NW Ireland. *J. geol. Soc. Lond.* **139**, 287–294.

Hutton, D. W. 1988. Granite emplacement mechanisms and tectonic controls: inferences from deformation studies. *Trans. R. Soc. Edinb., Earth Sci.* **79**, 245–255.

Hutton, D. W. & Reavy, R. J. 1992. Strike-slip tectonics and granite petrogenesis. *Tectonics* **11**, 960–967.

Lagarde, J.-L., Ait Omar, S. & Roddaz, B. 1990a. Structural characteristics of granitic plutons emplaced during weak regional deformation: examples from late Carboniferous plutons, Morocco. *J. Struct. Geol.* **12**, 805–821.

Lagarde, J.-L., Brun, J.-P. & Gapais, D. 1990b. Formation des plutons granitiques par injection et expansion latérale dans leur site de mise en place: une alternative au diapirisme en domaine épizonal. *C.r. Acad. Sci., Paris* **310**, 1109–1114.

Lagarde, J.-L., Dallain, C. & Capdevila, R. 1990c. Contexte tectonique de la fusion crustale post-épaississement dans le dôme anatectique du Velay (Massif Central Français). *C.r. Acad. Sci., Paris* **311**, 477–484.

Lagarde, J.-L., Capdevila, R. & Fourcade, S. 1992. Granites et collision continentale: l'exemple des granitoides carbonifères dans la chaîne hercynienne ouest-européenne. *Bull. Soc. géol. Fr.* **163**, 597–610.

Lagarde, J.-L., Dallain, C., Merle, O. & Ledru, P. 1993. Champs de déformation associés à l'expansion horizontale de magmas granitiques. Exemple des granites hercyniens du Velay, Massif Central. *C.r. Acad. Sci., Paris* **316**, 653–659.

Ledru, P., Dallain, C., Lardeaux, J. M. & Marignac, C. 1991. Tectonic evolution of the Velay granito-migmatitic dome, French Massif Central. *Terra Abs.* **3**, 204.

Ledru, P., Lardeaux, J. M., Santallier, D., Autran, A., Quenardel, J. M., Floc'h, J. P., Lerouge, G., Maillet, N., Marchand, J. & Ploquin, A. 1989. Où sont les nappes dans le Massif Central Français. *Bull. Soc. géol. Fr.* **3**, 605–618.

Lister, G. S. & Davis, G. A. 1989. The origin of metamorphic core complexes and detachment faults formed during Tertiary continental extension in the northern Colorado River region, U.S.A. *J. Struct. Geol.* **11**, 65–94.

Lister, G. S. & Dorsiepen, U. F. 1982. Fabric transition in the Saxony granulite terrain. *J. Struct. Geol.* **4**, 81–92.

Lister, G. S. & Williams, P. F. 1979. Fabric development in shear zones: theoretical controls and observed phenomena. *J. Struct. Geol.* **4**, 283–297.

Malavielle, J., Guihot, P., Costa, S., Lardeaux, J. M. & Gardien, V. 1990. Collapse of the thickened Variscan crust in the French Massif Central: Mont Pilat extensional shear zone and St. Etienne late Carboniferous basin. *Tectonophysics* **177**, 139–149.

Malavieille, J. & Taboada, A. 1991. Kinematic model for post-orogenic Basin and Range extension. *Geology* **19**, 555–558.

Mattauer, M., Brunel, M. & Matte, P. 1988. Failles normales ductiles et grands chevauchements. Une nouvelle analogie entre l'Himalaya et la chaîne hercynienne du Massif Central Français. *C.r. Acad. Sci., Paris* **306**, 671–676.

Matte, P. 1991. Accretionary history and crustal evolution of the variscan belt in Western Europe. *Tectonophysics* **196**, 309–337.

Merle, O. 1989. Strain models within spreading nappes. *Tectonophysics* **165**, 57–71.

Montel, J. M., Marignac, C., Barbey, M., Pichavant, P. 1992. Thermobarometry and granite genesis: the Hercynian low-P high-T Velay anatectic dome (French Massif Central). *J. metamorph. Geol.* **10**, 1–15.

Niorthe, D. 1990. Application du traitement d'image à la détermination d'indices de qualité de schistes ardoisiers. Unpublished D.E.A., Université de Rennes.

Pannozo, R. 1987. Two-dimensional strain determination by the inverse SURFOR wheel. *J. Struct. Geol.* **9**, 115–119.

Passchier, C. W. & Simpson, C. 1986. Porphyroclast systems as kinematic indicators. *J. Struct. Geol.* **8**, 831–843.

Paterson, S. R., Vernon, H. R. & Tobisch, O. T. 1989. A review of criteria for the identification of magmatic and tectonic foliations in granitoids. *J. Struct. Geol.* **11**, 349–363.

Ramsay, J. G. 1989. Emplacement kinematics of a granite diapir: the Chindamora batholith, Zimbabwe. *J. Struct. Geol.* **11**, 191–209.

Ramsay, J. G. & Graham, R. H. 1970. Strain variation in shear belts. *Can. J. Earth Sci.* 7, 786–813.

Schmid, S. M. & Casey, M. 1986. Complete fabric analysis of some commonly observed quartz *c*-axis patterns. In: *Mineral and Rock Deformation; Laboratory Studies—The Paterson Volume* (edited by Hobbs, B. E. & Heard, H. C.). *Am. Geophys. Un. Geophys. Monogr.* **36**, 263–286.

Schmid, S. M., Casey, M. & Starkey, J. 1981. An illustration of the advantages of a complete texture analysis described by the orientation distribution function (ODF) using quartz pole figure data. *Tectonophysics* **78**, 101–117.

Sibson, R. H. 1977. Fault rocks and fault mechanisms. *J. geol. Soc. Lond.* **113**, 191–213.

Simpson, C. & Schmid, S. M. 1983. An evaluation of criteria to deduce the sense of movement in sheared rocks. *Bull. geol. Soc. Am.* **94**, 1288–1291.

Spencer, J. E. 1984. Role of tectonic denudation in warping an uplift of low-angle normal faults. *Geology* **12**, 95–98.

Stel, H. 1991. Linear dilatation structures and syn-magmatic folding in granitoids. *J. Struct. Geol.* **13**, 625–634.

Van den Driessche, J. & Brun, J.-P. 1992. Tectonic evolution of the Montagne Noire (French Massif Central): a model of extensional gneiss dome. *Geodinamica Acta* **5**, 85–99.

Van der Molen, I. & Paterson, M. S. 1979. Experimental deformation of partially melted granite. *Contr. Miner. Petrol.* **70**, 299–318.

Vidal, P. 1980. L'évolution polyorogénique du Massif Armoricain: apport de la géochronologie et de la géochimie isotopique du Strontium. *Mém. S.G.M.B. Rennes* **21**.

Wdowinski, S. & Axen, G. J. 1992. Isostatic rebound due to tectonic denudation: a viscous flow model of a layered lithosphere. *Tectonics* **11**, 303–315.

Wernicke, B. & Burchfield, B. C. 1982. Modes of extensional tectonics. *J. Struct. Geol.* **2**, 105–115.